Journal of Civil Engineering
The Institution of Engineers, Bangladesh
Vol. CE 28, No. 2, 2000

LOCAL SCOUR AROUND BRIDGE PIERS UNDER THE ACTION OF VARIOUS WAVE-CURRENT COMBINATIONS

Md. Akhtaruzzaman Sarker[1], Noraieni Hj. Mokhtar[2] and Faridah Jaffar Sidek[2]

ABSTRACT : Estimation of maximum equilibrium scour depth around bridge is a very important factor for the design of pier foundations. Engineers are currently assessing scour conditions at existing bridges and also thinking to design new bridges that should be safe from scour. In this paper laboratory data for local scour around bridge piers are presented. The temporal variation of scour depth, effect of downflow on the maximum scour depth and the relationships of the relative scour depth with the Pier Froude Number are given. By analyzing the data, some empirical expressions are formulated to estimate the maximum scour depth around bridge piers for different wave-current combinations. It has been observed that the unidirectional current flow gives the higher scour rates than a combined wave-current condition.

KEYWORDS : Scour, bridge-pier, wave, flume.

INTRODUCTION

In recent years, many bridges are constructed to traverse straits and channels where both waves and currents interact with each other. Scour around structures founded to support the bridges is an important factor in order to ensure the stability of the structure. But there is a lack of standard judgement to measure the scour around coastal structures. Only limited investigations have been conducted on the mechanism of local scour around large-coastal structures.

Failures of structures due to scour hole development usually occur in extreme cases of unsteady flows interacting with a given structure and with changing channel conditions. If the alluvial stream becomes partially obstructed by a structure, the pattern in the channel around that structure is changed significantly. An understanding of the effect

1 Cranfield University, RMCS Shrivenham, Swindon, Wiltshire SN6 8LA, UK.
2 Coastal and Offshore Engineering Institute, University of Technology Malaysia, Jalan Semarak, 54100 Kuala Lumpur, Malaysia.

of these structures on the water flow around them is important in assessing the likely loading on the structure itself. It is also important in assessing the effect of resulting wake on any neighboring structures or on an erodible seabed.

Scour holes around bridge piers created by the flowing water is a major cause of bridge pier foundation failure. In order to reduce the huge cost involved in either over-designing the bridge foundation or rebuilding damaged bridges, a knowledge concerning the magnitude of the maximum scour depth and its relationship to different flow conditions is essential (Shen et al., 1966).

Local scour under clear-water or live-bed conditions has been a subject of considerable interest to researchers and bridge designers for many years. While the present understanding has improved and many empirical scour depth prediction formulae are available, such as the those summarized by Raudkivi (1986) and Sutherland (1986), vastly different results given by these formulae suggest that many aspects of scour are still not well understood. One fundamental aspect, which is the subject of the present study, is the maximum scour depth around bridge piers under current only, under combined current plus wave action and also under wave action only.

METHODS AND MATERIALS

The experimental set-up consists of a recirculating flume of length 16.10 m, width 0.90 m, and height 0.72 m. Fig. 1 shows a schematic layout of the flume. The flume is supported by steel framework. It includes tanks, pumps, sump and pipe networks. For the experimental work, a false bed made of plywood was set on the bottom of the flume. A portion of recess 3.5 m x 0.90 m x 0.20 m was provided in the middle of the flume as the test section. This test section was later filled with sand of medium size with a d_{50} of 0.80 mm, specific gravity(S_S) 2.64 and geometric standard deviations(σ_g) 1.20 Perspex sheets were fitted at the walls of the flume for levelling the sand. To direct the flow unidirectionally, 4 aluminum-sheet baffles of 1 m length were provided at a distance 1.5 m downstream of the wave paddle. An instrument carriage was mounted on the top of the flume. It could move in both longitudinal and transverse direction of the flume. It had also the arrangement to allow the specific instrument to move vertically. Scales were fitted in the flume, wherever necessary, to provide a reference datum. The adjustments for constant water depth and flow velocity were made by the control valve and the tailgate (overflow weir) fitted at the end of the flume.

Three-dimensional velocity components were measured by an Acoustic Doppler Velocimeter (ADV). It is a remote sensing 3-D velocity sensor which transmits acoustic pulses into the water and the pulses are scattered by the particles present in the water. A fraction of the energy returns toward the sound source. The echo is Doppler shifted in proportion to the particle velocity. This echo is then received by the receivers and the Doppler shift is calculated from the segments of the echo. Data were collected using ADV software. This raw data could then be converted using ADV data conversion program.

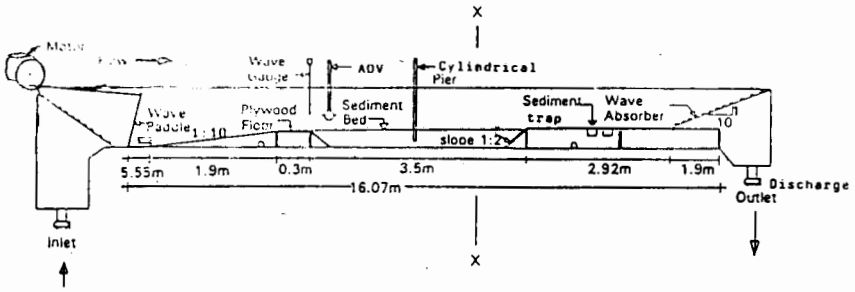

Fig 1. Schematic layout of the experimental flume

Wave was generated by a wave paddle of perspex sheet hinged to the flume bed at the inlet and linked to a motor via a metal rod. An artificial beach made of wire meshes topped with some fibrous materials and tied on an inclined wooden slope was placed at the end of the flume to absorb wave energy and thereby minimize wave reflection. Wave reflection coefficient of the flume was determined and was found to be 6.4 per cent. A screen made of wire mesh was also used in front of the wavemaker to damp lateral oscillations. To avoid initial bed erosion, blocks of bricks were placed across the flume just after the recess in order to slow down the water which shoots out from the stilling basin. Bricks were removed once an adequate flow depth was attained in the flume. After each run, a wooden block was used to level the sand bed. Sediment traps were incorporated at the downstream end of the test section to collect the transported sand, if any. The discharge pipe was controlled by valve to slow down the

retreating water whenever necessary and safeguard the final topography of the scoured bed against damage. The experiment was carried out using cylindrical steel pipes with diameters, D_1 = 33 mm, D_2 = 60 mm and D_3 = 89 mm to represent a small scale model of a bridge piper. The model was placed vertically at the centerline of the section.

RESULTS AND DISCUSSIONS

Tempord variation of scour depth

(a) Current action only

Figure 2 shows the temporal variation of scour depth for different flow depths. From this figure the following observations coued be made :

i) Scour depth increases with the increase of approach flow velocity.

ii) The rate of increase in scour depth is high initially, up to one and a half hour from the commencement of the test. After this, the scour depth also increases but with a decreased rate. After about three hours from the beginning of the test, scour hole attains to an equilibrium condition.

iii) The rate of increase of scour depth at the initial stage is higher than that of the approach flow. This rate then decreases gradually.

(b) Current and wave action

Figure 2 illustrates the temporal variation of scour depth for different flow depths for the combined case. This figure indicates that the depth of scour hole increases with the increase of elapsed time. The rate of increase is higher, up to two hours from the commencement. After this, the depth also increases but at a very reduced rate showing almost the equilibrium condition of the hole. For the higher flow depth i. e., for the lower velocity, the figure changes its pattern remarkably. Here at the very beginning stage of scouring, the depth increases with the increase in the elapsed time. After about half an hour, the depth of the hole reduces. Again it starts to increase at a very low rate. After two hours from the beginning of the test, the scour hole reaches equilibrium.

(c) Wave action only

As shown in Fig. 2, initially higher scour depth is observed. This scour depth then reduces at a higher rate as the time is elapsed. But after one hour from commencement the rate reduces. It takes about two and a half hours to reach an equilibrium.

Topography of the scoured bed

(a) Current oaction only

The bed scour studies for 'current only' have led to the following observations , as depicted is Fig. 3

i) The higher the approach flow velocity, the deeper the scour depth.

ii) The higher the approach flow velocity, the wider the scour depth.

iii) The higher the approach flow velocity, the longer is the distance before the bed gains it original level at the downstream.

iv) There is a secondary hole at the downstream side. With higher flow velocity, the secondary scour hole becomes clear at the downs treqm.

Typical 3-D scoured bed diagram for D=60 mm and h=250 mm is shown in Fig. 4.

(b) Current plus wave

The maximum scour depth is formed at the upstream side closer to the pier. The shape of the scour hole at the upstream side is almost similar to that for 'current only' case. But at the downstream side up to about 16.5 pier diameters from the pier, there are ripples formed with a width of 2 pier diameters at the near end and 7.5 pier diameters at

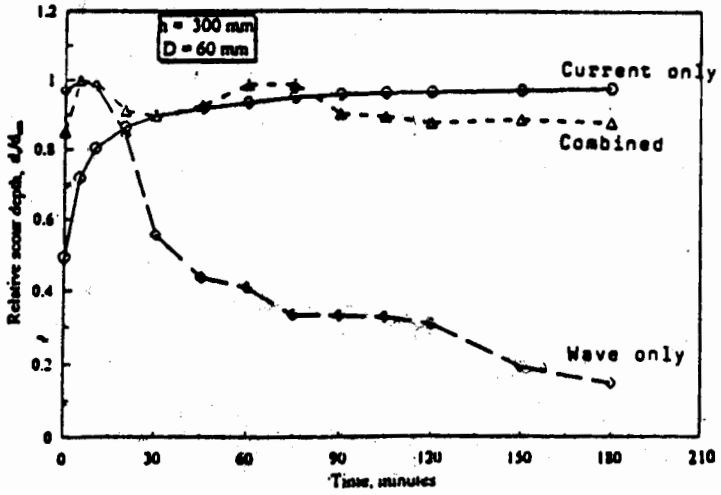

Fig 2. Temporal variation of scour depth for different wave-current combinations for D = 60 mm and h = 300 mm

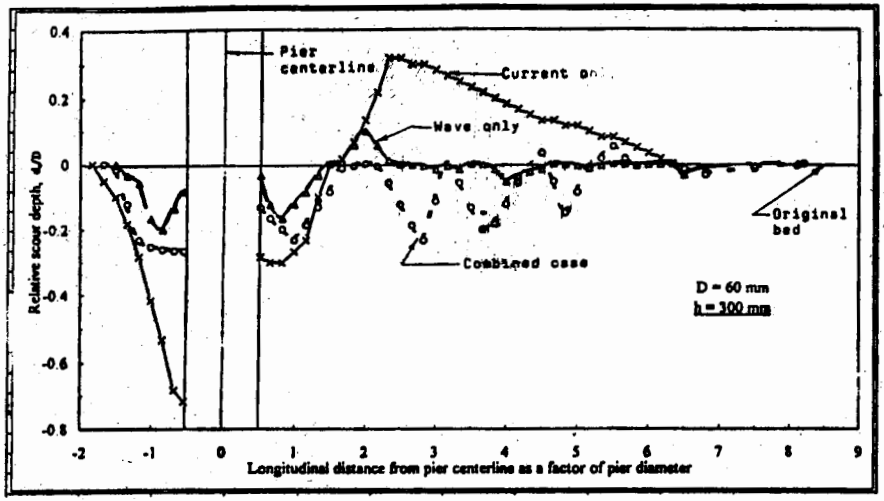

Fig 3. 2-D diagram of scoured bed for different wave-current combination for D = 60 mm and h = 300 mm

the rear end. These ripples are bent at about 45 degrees from the centerline of the flume towards the flume wall. But while the applied current is weak, the maximum scour depth is found to occur at a point of 1.3 pier diameters downstream and 1.5 pier diameters on the lateral side from the pier. In this case, ripples are observed between the distance of 10.5 pier diameters and 16.5 pier diameters at the downstream of the pier.

(c) Wave action only

In the case of 'wave only', the maximum scour depth is observed at the downstream end of the pier. (shown in Fig. 3)

Effect of downflow on the maximum scour depth

Figure 5 illustrates the relationships between the relative maximum scour depth and the downflow as a fraction of the mean flow velocity for three different wave-current combinations. A linear relationship is obtained for the maximum scour depth and the downflow for the current with and without wave cases. Lower rate of

increase of maximum scour depth with the increase of downflow is observed for the current only case. The rate of increase of the maximum scour depth for the combined case is higher as shown in Fig. 5.

Expressions are derived to estimate the maximum scour depth as a function of downflow for different wave-current combinations from the above mentioned plot. These equations are as follows :

i) $d_{sm}/D=0.36e^{1.83(w/U)}$ $R^2=0.98$ for current only (1)

ii) $d_{sm}/D=0.16e^{2.71(w/U)}$ $R^2=0.96$ for combined case (2)

iii) $d_{sm}/D=0.34(w/U)^{0.65}$ $R^2=0.83$ for wave only (3)

Effect of approach velocity magnitude on the maximum scour depth

Figure 6 illustrates the relationships between the maximum scour depth (d_{sm})/Pier diameter(D) ratios as a function of the Pier Froude Number [$\mathbf{F} = U/\sqrt{(gD)}$] for different wave-current combinations. For the current only case, the rate of increase of the maximum scour depth is lower. The rate of increase of d_{sm}/D for the combined case is higher as depicted in Fig. 6.

The acceleration due to gravity, g is constant for the present study. So, the Pier Froude Number, **F** varies with only the undisturbed approach flow, U and pier diameter, D. So, from Fig. 6, it is clear that the maximum scour depth increases with the increased undisturbed approach flow. This plot shows good agreement with that developed by Shen et. al (1969) for current only case. In this figure, the present study has given a slightly flatter gradient due to the smaller pier and larger sediment size used.

Expressions are derived to estimate maximum scour depth as a function of the Pier Froude Number, **F** for different wave-current combinations. These equations are as follows :

i) $d_{sm}/D=4.49\mathbf{F}+0.03$ $R^2=0.99$ for current only (4)

ii) $d_{sm}/D=4.01\mathbf{F}^{1.23}$ $R^2=0.98$ for combined case (5)

iii) $d_{sm}/D=0.6e^{9.49F}$ $R^2=0.97$ for wave only (6)

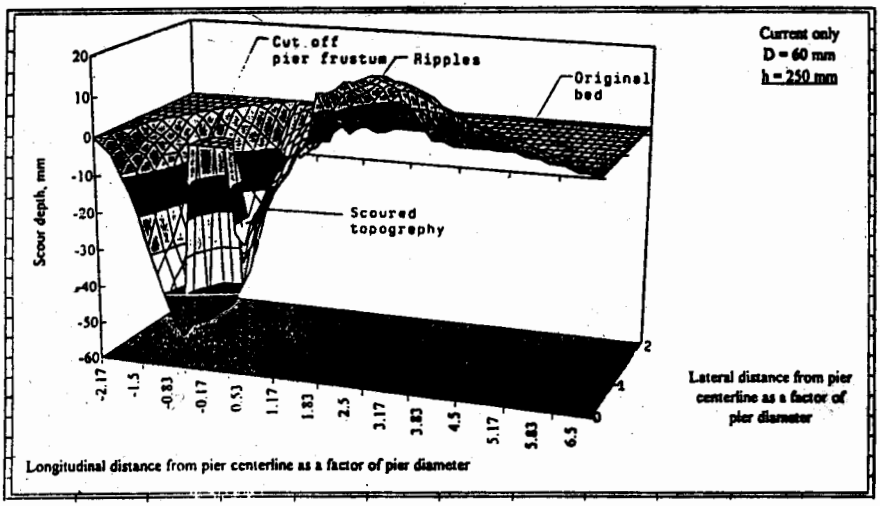

Fig 4. 3-D diagram of the scoured bed topography for current flow only for D = 60 mm and h =250 mm

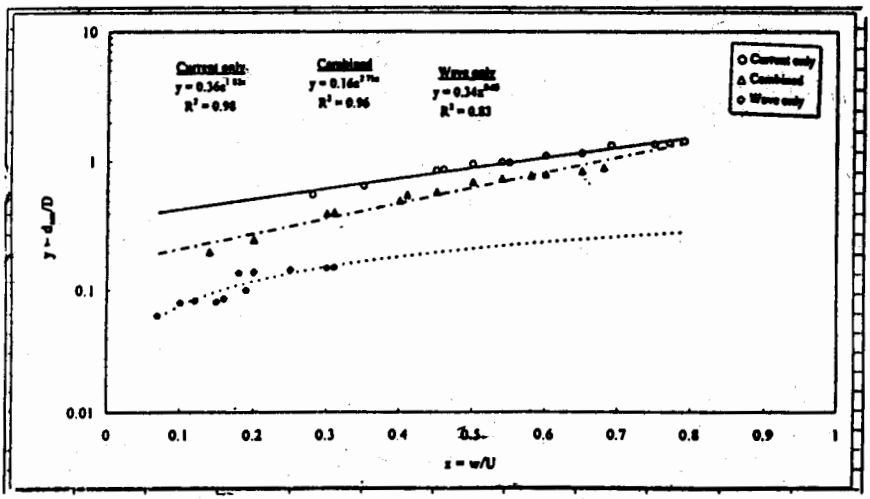

Fig 5. Effect of downflow on the maximum scour depth

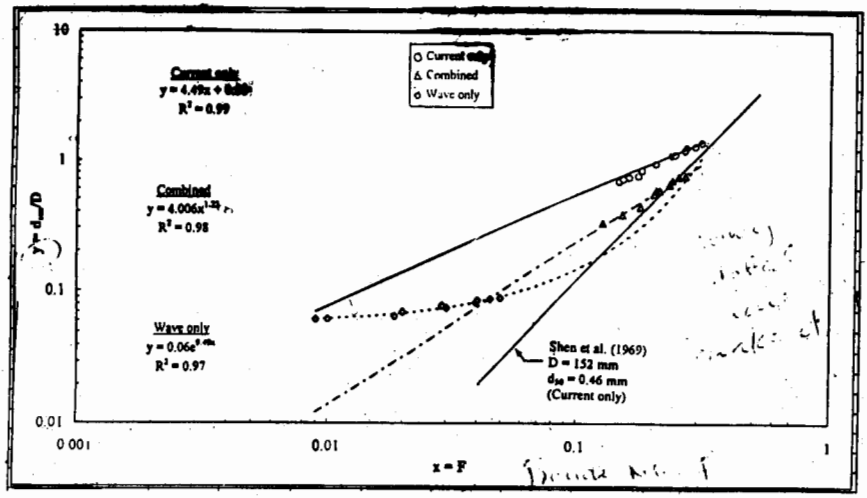

Fig 6. Maximum scour depth - Pier diameter ratios as a function of Pier Froude Number

CONCLUSION

The depth of the maximum scour increases with the increased undisturbed mean approach flow for both current only and the combined case. The rate of increase is higher for the current only case. For the current only case, the scour depth initially increases with increased downflow. For the combined case the scour depth also increases with the increased downflow. The maximum scour depth increases with the increased downflow for the three different current - wave combinations. For the current only case, this rate of increase is the highest one, for the combined case it is the intermediate and for the wave only case this rate is the lowest. Scour depth for current only case increases with the elapsed time. Initially this rate of increase is higher. Afterwards, it is also increased but with a decreased rate. Finally, it comes to an equilibrium. For the combined case, the scour depth increases with elapsed time. Initially the rate of increase is higher.

Deeper and wider scour depth was found for higher approach flow velocity. For higher approach flow velocity, it takes a longer distances for the bed to attain its original level at the downstream. The higher the approach flow, the more clear the secondary hole at the downstream. Maximum scour depth is found at the upstream of the pier for current only case, but the combined case shows a tendency to form it towards the downstream. For the wave only case, the maximum scour depth is found at the downstream. The wave related field shows the formation of ripples at the downstream where the current only case shows the formation of dunes at the same side.

REFERENCES

Raudkivi, A. J. (1986). "Functional trends of scour at bridge piers". Journal of Hydraulic Engineering, Vol, 112, No. 1, pp. 1-13.

Shen. H. W., Schneider V. R. and Karaki, S. S. (1966), "Mechanics of local scour". Civil Engineering Department Research Center, Colorado State University, Fort Collins, Colorado.

Sutherland, A. J. (1986), "Reports on bridge failure". R.R.U. Occasional paper, National Roads Board, Wellington, New Zealand.

NOTATION

D pier diameter, mm
ds scour depth, mm
d_{sm} maximum scour depth, mm
d_{50} sediment mean diameter, mm
F Pier Froude Number
h flow depth, mm
U mean velocity
w downflow component, mm/sec